Talanta 237 (2022) 122912

Contents lists available at ScienceDirect

Talanta

journal homepage: www.elsevier.com/locate/talanta

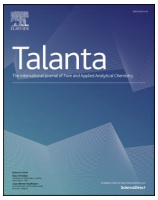

Rapid analysis of quinones in complex matrices by derivatization-based wooden-tip electrospray ionization mass spectrometry

Chen Ling [a], Qiaofang Shi [a], Zhanpeng Wei [a], Jingjing Zhang [a], Junjie Hu [a], Jiying Pei [a,b,*]

[a] School of Marine Sciences, Guangxi University, Nanning, Guangxi, 530000, PR China
[b] Coral Reef Research Center of China, Nanning, Guangxi, 530000, PR China

ARTICLE INFO

Keywords:
Wooden-tip electrospray ionization
Quinones
Derivatization
Mass spectrometry
Complex matrices

ABSTRACT

Quinones are important components participating in various biological processes as well as hazardous substances to human health. Rapid determination of quinones in environmental samples and biofluids is the basis for assessing their health effect. Here, we presented a rapid, straightforward, highly sensitive and environmental-friendly wooden-tip electrospray ionization mass spectrometry (ESI-MS) method for the determination of quinones in PM2.5, urine and serum. An amine group "tag" was introduced to the quinone structure through *in situ* derivatization with cysteamine to improve ionization efficiency of quinones in wooden-tip ESI-MS. The toothpicks were treated by sharpening and acidification with HNO_3. Experimental parameters, including sample volume, spray voltage, and spray solvent composition were optimized to be 1 μL, 3.5 kV, and ACN/$CH_3COOC_2H_5$ (*v*/*v*, 9:1), respectively. The limits of detection for the determination of 1,4-benzoquinone, methyl-*p*-benzoquinone, 1,4-naphthoquinone and 1,4-anthraquinone in ACN under the optimal conditions were 1.00, 0.96, 0.13, 0.16 ng (1.00, 0.96, 0.13, 0.16 μg/mL, sample volume, 1 μL), respectively. This approach was successfully applied to the determination of 1,4-naphthoquinone and 1,4-anthraquinone in complex matrices, including PM2.5, urine and serum without or with minimal sample preparation (LOD range: 0.22–1.48 ng).

1. Introduction

Quinones are a class of important compounds participating in various biological processes. For example, quinone can induce heme oxygenase-1 in aortic endothelial cells to protect the vessel [1]. In addition, quinones are harmful to human health by generating reactive oxygen species (ROS) to exert a variety of hazardous effects, including acute cytotoxicity, immunotoxicity, and carcinogenesis [2–4]. It has been illustrated that quinones can lead to mutations and cancer as well as inhibit enzyme activity. Polycyclic aromatic hydrocarbons quinone (PAHQ), a type of common constituents found in airborne particulate matter (PM), is known as the products of incomplete combustion of fuels (such as petroleum, coal and cigarettes) or chemical reactions of PAHs with ozone and radical species in the atmosphere [5–7]. Quinones in environmental and biological samples are indicators to assess human exposure. For example, 9,10-dihydroxyphenanthrene (9,10-PQHG), the metabolite of phenanthrenequinone (9,10-PQ), was found as a biomarker of PAHQ exposure, and was detected in the urine from nonoccupationally-exposed individuals who lived in a suburban area [8]. Developing a rapid, cost-effective method to quantify quinones in environmental samples and biofluids is thus of great importance for routine assessment of quinone exposure.

Quinones are traditionally determined by fluorescence [9–11], chemiluminescence (CL) [12], gas chromatography-mass spectrometry (GC-MS) [13–15] and liquid chromatography-mass spectrometry (LC-MS) [16,17]. Among these techniques mass spectrometry is the most widely used due to high sensitivity and specificity. However, sample pretreatment processes are usually time-consuming and labor-intensive in GC-MS and LC-MS, and require the usage of organic solvent, which can produce secondary environmental pollution. Thus, environmental-friendly methods for determining quinones in complex matrices are still in great demand.

Ambient mass spectrometric techniques have received considerable attention in the past decade as they allow *in situ* analysis with minimal sample pretreatment. The first ambient ionization source, desorption electrospray ionization (DESI), was developed by Cooks' group in 2004 [18]. Since then more than 30 ambient ionization techniques, including direct analysis in real time (DART) [19], extractive electrospray ionization (EESI) [20], laser ablation electrospray ionization (LAESI) [21], and paper spray ionization [22,23], have been developed. Wooden-tip

* Corresponding author. School of Marine Sciences, Guangxi University, Nanning, Guangxi, 530000, PR China.
E-mail address: pjying@gxu.edu.cn (J. Pei).

https://doi.org/10.1016/j.talanta.2021.122912
Received 1 June 2021; Received in revised form 27 September 2021; Accepted 29 September 2021
Available online 4 October 2021

electrospray ionization mass spectrometry (ESI-MS) is a novel electrospray ionization-based ambient technique that can be used for quantitative and qualitative analysis of compounds in complex matrices [24]. In wooden-tip ESI-MS, a small amount of sample is loaded onto the toothpick tip, and subsequently high voltage is applied to migrate and ionize compounds in the sample. Wooden-tip ESI-MS offers enormous advantages, including convenient sampling, low demand of sample amount, and high resistance to matrix interference, making this novel technique a greater player in performing rapid tests when compared to traditional MS-based approaches. Today, wooden-tip ESI-MS has been extensively applied in analyzing compounds in various types of samples, such as body fluid [25–27], pharmaceuticals [28,29], food [30,31] and plant materials [32,33].

Herein, we developed a straightforward and highly sensitive wooden-tip ESI-MS method for the rapid determination of quinones in complex matrices. Ionization of quinone in wooden-tip ESI-MS was boosted by *in situ* derivatization with cysteamine that brought an amine tag to the quinone structure. Four quinones (1,4-benzoquinone (BQ), methyl-*p*-benzoquinone (MBQ), 1,4-naphthoquinone (NQ) and 1,4-anthraquinone (AQ)) were chosen as the model compounds to optimize experimental conditions and to evaluate quantitative performance including linearity, relative standard deviation (RSD) and limits of detection (LOD). Finally, the method was applied to the determination of quinones in PM2.5, urine and serum without or with minimal sample preparation to demonstrate its wide applicability.

2. Experimental

2.1. Chemicals and materials

BQ, MBQ, NQ, AQ, 1,4-benzoquinone-d_4 (BQ-D_4) and 1,4-naphthoquinone-d_6 (NQ-D_6) were purchased from ANPEL Laboratory Technologies Inc. (Shanghai, China). The molecular structures of quinones were listed in Table 1. Cysteine and glutathione were purchased from Sangon Biotech Co. (Shanghai, China). Cysteamine was purchased from J&K Scientific Ltd. (Beijing, China). HPLC grade methanol, acetonitrile and ethyl acetate were purchased from Burdick & Jackson Inc. (Muskegon, MI, USA). The deionized water (resistivity: 18.2 MΩ·cm) was prepared with Milli-Q water-purification system (Millipore, MA, USA). The solutions used in this experiment were all prepared in acetonitrile (ACN) unless otherwise noted.

Wooden toothpicks were purchased from a local supermarket (Guangxi, China). PM2.5 samples were taken from May 26 to 27, 2019, at Guangxi University (Guangxi, China). The air was drawn through a quartz fiber filter (20.3 cm × 12.7 cm, Munktell) by a PM2.5-PUF-300 active atmospheric sampler (Guangzhou Mingye Huanbao Technology Company, Guangzhou, China) with a sampling flow rate of 300 L/min and duration of 24 h. Human urine samples were donated by one healthy volunteer with IRB approval. Serum samples were purchased from Sangon Biotech Co. (Shanghai, China). PM2.5, urine and serum samples were stored at −20 °C.

2.2. Mass spectrometry

All experiments were carried out with an LTQ mass spectrometer (Thermo Scientific, San Jose, CA, USA). All mass spectra were obtained in positive ion mode. The inlet temperature was set at 275 °C. For tandem mass spectrometry (MS/MS), helium was used as the collision gas, the collision-induced dissociation (CID) energy was set at 35% with an activation time of 30 ms, and the isolation width was set as *m/z* 1.0. The other mass spectrometer parameters used in the experiment were default values.

2.3. Pretreatment of toothpick

The toothpick tip was sharpened to the ultimate diameter of 0.1 mm (Fig. S1). The toothpicks were treated with HNO_3 solution following Su's method [34]. Briefly, the toothpicks were soaked in 10^{-3} M HNO_3 solution (maintained in a 45 °C water bath) for 3 h, then washed five times with deionized water, and dried at 70 °C in an oven. The prepared toothpicks were stored in a chamber with constant temperature and humidity.

2.4. Pretreatment of quartz fiber filter with PM2.5

The quartz fiber filter after being used to collect PM2.5 was weighed and cut into six fragments with the same size (5 cm × 5 cm), and added with different amounts of quinones solution (0, 50, 100, 200, 500, 1000 μL of 1000 μg/mL stock solution). After drying for 1.5 h at room temperature, the filter membranes were cut into pieces and placed in the 15 mL centrifuge tube. Subsequently, 10 mL of ACN was added for extraction by ultrasonication combined with vortex oscillation for 30 min.

2.5. Home-made ESI setup

The home-made ESI consisted of a syringe (1700 series, Hamilton, NV, USA), a 50 cm long etched fused-silica capillary (100 μm i.d., 365 μm o.d.) and a tee-junction to assist the nebulization of sample solution [35]. The distance between the fused-silica capillary tip and the inlet of mass spectrometer was 1 cm. Nitrogen was used as sheath gas and the voltage was set as 3.5 kV. The reaction solution of quinone and sulfhydryl reagents in the syringe flowed through the fused-silica capillary with a flow rate of 2 μL/min.

Table 1
The structures of quinones and the major characteristic fragment ions of the derivatives.

Quinones	Molecular structure of quinones	Molecular structure of derivatives	*m/z* of derivatives parent ion	*m/z* of derivatives characteristic fragments ion
BQ		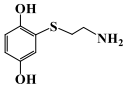	186	169
MBQ		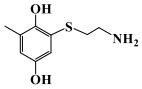	200	183
NQ		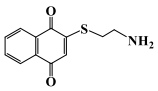	234	217
AQ	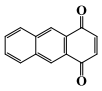	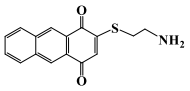	284	267

3. Results and discussion

3.1. Optimization of the experimental conditions

Quinones are compounds absent of basic and acidic sites and thus have low ionization efficiency in electrospray-based ionization sources. It has been illustrated that their ionization efficiency could be improved by introducing an amine group with strong proton-binding ability into the molecular structures [36]. We tested three sulfhydryl reagents (cysteine, glutathione, and cysteamine) as derivatization reagents, and found that the cysteamine derivatives showed the best signals in ESI-MS (Fig. S2-S3). Therefore, cysteamine was chosen as derivatization reagent in the following experiments. The diagram of the wooden-tip ESI-MS experimental setup was shown in Fig. 1. One μL of quinone solution and 2 μL of cysteamine solution were sequentially added onto the toothpick tip, where quinones were derivatized *in situ*. High voltage was applied after drying of the toothpick, then the spray solvent was added to initiate the electrospray and ionization.

In the MS/MS spectra of quinone derivatives, dominant fragment ions indicated to neutral loss of an ammonia from quasimolecular ions (*i.e.* fragment ions of *m/z* 169, 183, 217 and 267 for BQ, MBQ, NQ, and AQ derivatives, respectively) and were used for quantification of quinones. For NQ and AQ derivatives, their MS/MS spectra showed fragment ions of $[M-34]^+$ and $[M-60]^+$, which were speculated to be $[M-H_2S]^+$ and $[M\text{-}CH_2CH_2SH]^+$ (Fig. S4). The MS^3 spectra of $[M-17]^+$ fragment ions of NQ and AQ derivatives showed loss of a water, a carbon dioxide and a sulfydryl group (Fig. S5). The presence of $[M-H_2S]^+$ and $[M\text{-}CH_2CH_2SH]^+$ ions in the MS/MS spectra and $[M-HS]^+$ in the MS^3 spectra suggested that NQ- and AQ-derivatives were possibly subject to intramolecular rearrangements in the CID process. This phenomenon was understandable as intramolecular rearrangement commonly occurred in CID [37–40], such as the elimination of SO_2 from aromatic sulfonamides [39] and NH_3 from dibenzylamine [40].

On the other hand, BQ- and MBQ-cysteamine derivatives showed parent ions at *m/z* 186 and 200, respectively. Meanwhile, $[M-H_2S]^+$ and $[M\text{-}CH_2CH_2SH]^+$ were not observed in their MS/MS spectra. This implied that the structures of BQ- and MBQ-cysteamine derivatives were reduced into the diphenol form, while the quinone structures were preserved in NQ and AQ derivatives. The structure differentiation of four quinone derivatives might be explained by their reduction potentials. The reduction potentials of BQ, MBQ, NQ, and AQ are −0.851, −0.928, −1.029, and −1.259 V, respectively [41]. In fact, compounds with higher reduction potentials (less negative values) were more prone to be reduced. It was also reported that BQ and MBQ-glutathione derivatives could be reduced by severe corona discharge during positive ESI-MS while NQ- and AQ-glutathione derivatives could not [42], which is in accordance with our study. To sum up, the molecular structure, parent ion and characteristic fragment ion of the derivatives were listed in Table 1. It is noteworthy that in-source fragment (deamination) of four quinone derivatives was observed, and the fragment extents had the tendency of BQ > MBQ > NQ > AQ (Fig. S4A). Therefore, though the ionization efficiencies of four quinone derivatives were similar, their absolute signal intensities had the tendency of BQ < MBQ < NQ < AQ.

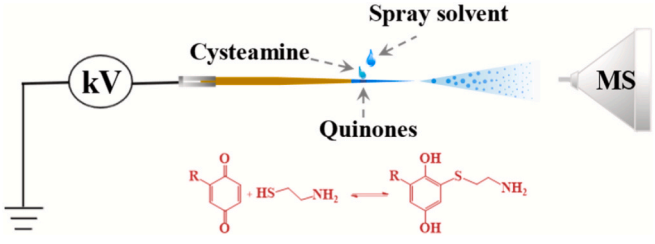

Fig. 1. Diagram of wooden-tip ESI-MS for quinone determination. (Coloured in print.)

Then the experimental conditions were optimized for the quantitative analysis of quinones. First, we compared the effect of the way to modify toothpicks on quinones determination. It is reported that the impurities in the toothpick resulted in complex background signal and suppressed the signal of target compounds. However, treatment by HNO_3 and NaClO could alter the lignin fiber structure, and thus effectively eliminated the interference of impurities [34]. On the other hand, sharpening the toothpick could strengthen the signal intensity of quinone derivatives, which could be attributed to the efficient formation of Taylor cone by enhancing electric field [24,43,44]. Therefore, the toothpick was treated by soaking in HNO_3 solution (10^{-3} M) and sharpening before the MS experiment. However, the sequence of acidizing and sharpening of the toothpick would affect the ionization efficiency. As shown in Fig. 2A, the sequence of sharpening→acidizing worked better than the sequence of acidizing→sharpening for all four quinones. We speculated that toothpicks were more readily permeated by HNO_3 after sharpening, resulting in more efficient oxidization of the internal impurities. Therefore, the sequence of sharpening→acidizing was used to treat toothpicks in the following experiment.

Sample volume affects the signal intensity of quinone derivatives during wooden-tip ESI-MS. One μL and 2 μL of sample were compared in this experiment. Higher signal intensity and better repeatability were obtained with 1 μL of sample (Fig. 2B). With the addition of 2 μL of sample onto the toothpick tip, the solution diffused around the tip visually, resulting in weak signal intensity and poor repeatability. Oppositely, a sampling volume of less than 1 μL was less accurate with a pipettor, and it is hard to add it onto the toothpick tip. Therefore, we chose 1 μL as the sample loading volume.

Spray voltage is another parameter affecting the signal intensity of quinone derivatives during wooden-tip ESI-MS. We compared 3 kV, 3.5 kV, 4 kV, 4.5 kV, and 5 kV here. As shown in Fig. 2C, the highest signal intensities were obtained with the spray voltage of 3.5 kV. In fact, spray current, which is generated after application of voltage, is proportional to the amount of charged droplets; thus higher spray voltage results in higher signal intensity. However, a spray voltage that is too high can also induce severe corona discharge that can result in both poor signal intensity and instrument damage [35,42]. Though visual observation of corona discharge generally occurs above 4 kV during ESI [45], extensive investigations have indicated that corona discharge could occur at low spray voltage before the visual observation of light emission by monitoring current-voltage curve [46]. Decreased signals of quinone derivatives were observed with spray voltage higher than 3.5 kV during

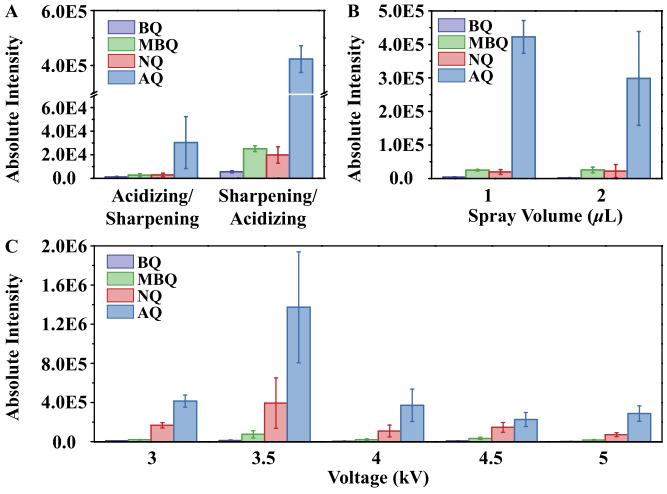

Fig. 2. The effect of the A) sequence of toothpick modification, B) sample volume, C) spray voltage on the signal intensities of BQ, MBQ, NQ and AQ derivatives during wooden-tip ESI-MS. The error bars represent the standard deviation of three repeated measurements.

the wooden-tip ESI-MS. We speculated that this might be due to the occurrence of corona discharge on the artificially sharpened toothpick tip. Thus, the optimal spray voltage was set as 3.5 kV.

The composition of spray solvent affects the extraction, transfer and ionization of target compounds from the toothpick [47], and the amount of spray solvent affects the efficient formation of Taylor cone. Ten μL of ACN/$CH_3COOC_2H_5$ (v/v, 9:1) was chosen as the spray solvent after optimization of these parameters (Fig. S6-S7).

3.2. Evaluation of the analytical performance

Under the optimal conditions, the analytical performance of wooden-tip ESI-MS for BQ, MBQ, NQ and AQ determination was evaluated. Unsatisfactory quantitative ability and poor reproducibility are two of the greatest analytical challenges of ambient ionization sources [48]. Taking spray-based ambient ionization source as an example, the quantitative performance is mainly affected by spray instability, which results in scan-to-scan fluctuation of the ion current. This problem can be solved by the introduction of internal standards whose signals can be used to calibrate spray instability. Here, 10 ng BQ-D_4 was added as the internal standard for BQ and MBQ determination, and 10 ng NQ-D_6 was added as the internal standard for NQ and AQ determination. The internal standards were added into the quinone solution before sampling. The calibration curves were linear in the concentration range of 1–50 μg/mL for the four quinones, with R^2 being 0.989, 0.996, 0.998 and 0.993 for BQ, MBQ, NQ and AQ, respectively (Fig. 3). Though the absolute signal intensities of four quinone derivatives had the tendency of AQ > NQ > MBQ > BQ, the ratios of the signal intensities of quinones and the internal standards had the tendency of AQ ≈ MBQ > NQ ≈ BQ. LODs were calculated based on three times the standard deviation of 11 blank values ($3 \times \delta_{blank}/k$, *k is the slope of the linear equation*), and they were 1.00, 0.96, 0.13 and 0.16 ng (1.00, 0.96, 0.13, 0.16 μg/mL, sample volume, 1 μL) for BQ, MBQ, NQ and AQ, respectively (Table S1). With the usage of internal standards, the relative standard deviations (RSDs) of the four quinones at most concentrations were below 30%, with individual exceptions with RSDs over 30% at low concentrations. This might be due to the large signal fluctuation at low concentrations and few measurement repetitions (n = 3). We suggest that the repeatability can be further improved by using an automatic platform to sharpen the toothpick tip and automatic sampling [48].

3.3. Detection of quinones in complex matrices

PM2.5, urine and serum were chosen to test the ability of wooden-tip ESI-MS for determination of quinones in complex matrices. After addition of four quinones in the real samples, they were analyzed by wooden-tip ESI-MS. As shown in Fig. 4, the signal peaks of NQ and AQ derivatives were observed in the full scan mass spectrum for the PM2.5 sample. Their identifications were also verified by the MS/MS spectra (inset of Fig. 4). The R^2 for NQ and AQ determination in PM2.5 in the concentration range of 5–100 μg/mL were 0.962 and 0.992, respectively, with LODs being 0.22 and 0.31 ng (0.22 and 0.31 μg/mL, sample volume, 1 μL), respectively (Fig. 5A). Good linearity was also achieved for NQ and AQ determination in urine and serum (Fig. 5B and C). The LODs of NQ and AQ in urine were 0.65 and 1.48 ng (0.65 and 1.48 μg/mL, sample volume, 1 μL), respectively, while those in serum were 0.24 and 0.98 ng (0.24 and 0.98 μg/mL, sample volume, 1 μL), respectively. However, BQ and MBQ were not successfully quantified in PM2.5, urine, and serum. Bolton et al. reported that BQ could target various biological substances, such as metal ions, peptides, proteins, and DNA in organisms [4,49]. We speculated that BQ and MBQ might react with various substances in PM2.5, urine, and serum, and thus were hardly observed due to their low concentrations and also severe ion suppression by high concentration of salts in samples. To support this speculation, we observed urine samples that were spiked with BQ and MBQ and stored in dark room for 3 h, and found that the urine darkened gradually (Fig. S8). In addition, NQ and AQ were not detected in real PM2.5 sample, possibly due to weak pollution of the sampling position, campus of Guangxi University, which is far away from coal combustion or factory emission.

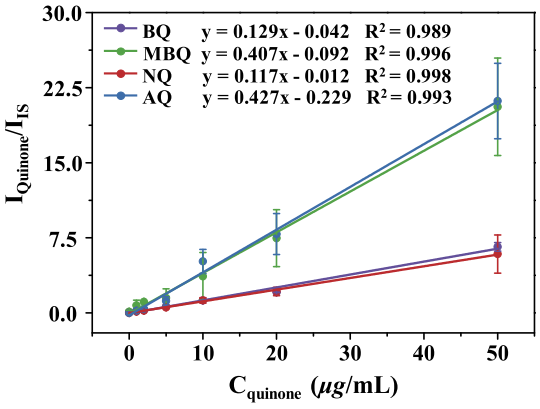

Fig. 3. The linear dynamic curves for BQ, MBQ, NQ and AQ determination in ACN/$CH_3COOC_2H_5$ (v/v, 9:1) by wooden-tip ESI-MS. BQ-D_4 (10 ng) was used as the internal standard for BQ and MBQ determination, and NQ-D_6 (10 ng) was used as the internal standard for NQ and AQ determination. IS was internal standard. The error bars represent the standard deviation of three repeated measurements.

4. Conclusions

This study demonstrated that wooden-tip ESI-MS could be an alternative for the rapid determination of quinones in complex matrices, such as PM2.5, urine and serum without or with minimal sample preparation (only a few extraction steps were needed for PM2.5 analysis before wooden-tip ESI-MS determination). Sample loading volume, voltage, and spray solvent composition were optimized to be 1 μL, 3.5 kV, and ACN/$CH_3COOC_2H_5$ (v/v, 9:1), respectively. Under optimal conditions, good linearity and repeatability were achieved for BQ, MBQ, NQ and AQ determination. The LODs for the determination of BQ, MBQ, NQ and AQ in ACN were 1.00, 0.96, 0.13 and 0.16 ng (1.00, 0.96, 0.13, 0.16 μg/mL, sample volume, 1 μL), respectively. In addition, good linearities and repeatability were achieved for NQ and AQ determination in PM2.5, urine and serum. The LODs for NQ and AQ determination in PM2.5, urine, serum were 0.22 and 0.31 ng, 0.65 and 1.48 ng, 0.24 and 0.98 ng (0.22 and 0.31, 0.65 and1.48, 0.24 and 0.98 μg/mL, sample volume, 1 μL), respectively. Compared with other ambient ionization methodologies for quinone determination in complex matrices, such as paper spray ionization [50], our wooden-tip ESI-MS method showed higher sensitivity, lower sample consumption and wider applicability to more

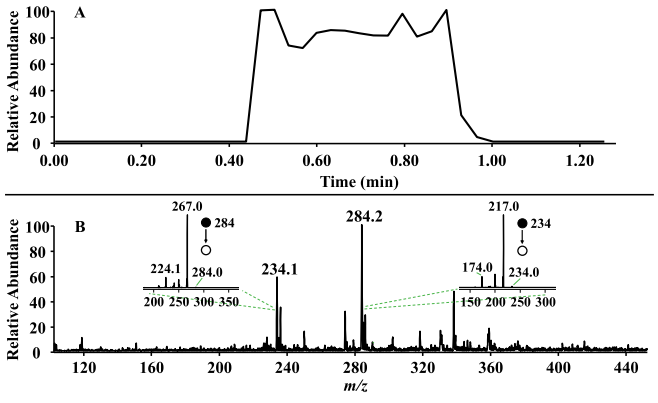

Fig. 4. A) Total ion chromatogram (TIC) and B) the corresponding mass spectrometry for NQ and AQ determination in PM2.5by wooden-tip ESI-MS.

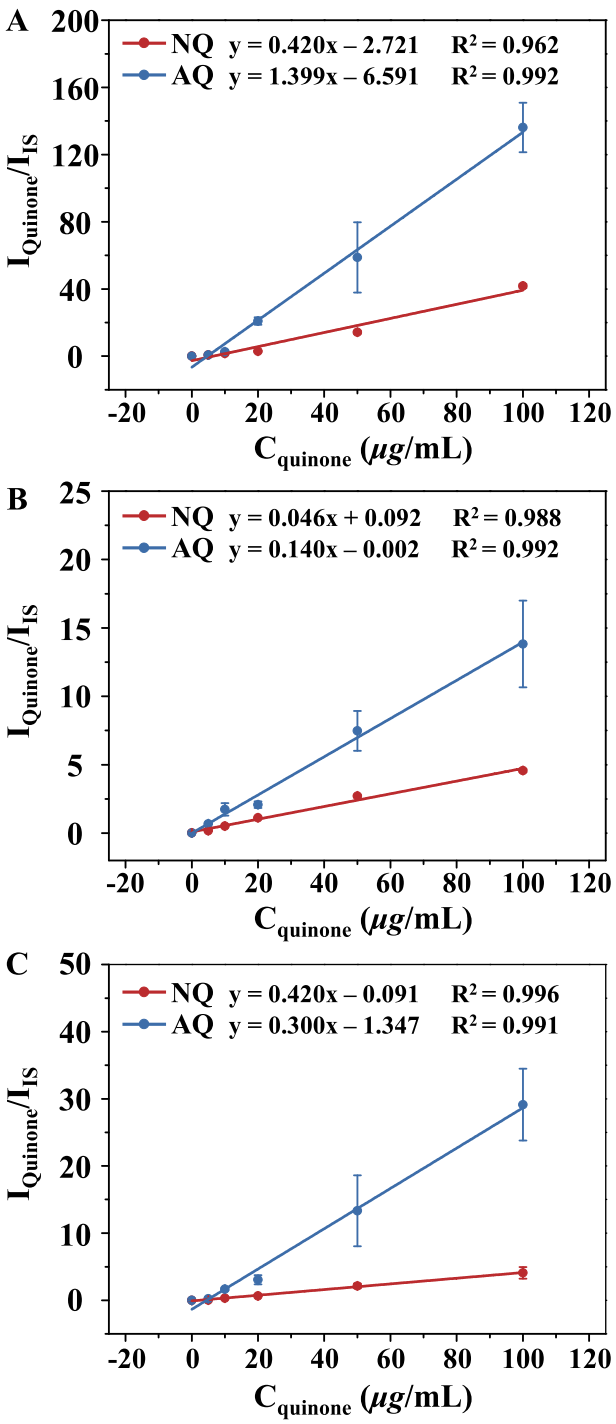

Fig. 5. The linear dynamic curves for NQ and AQ determination in A) PM2.5, B) urine, and C) serum by wooden-tip ESI-MS. Twenty, 30, and 30 ng of NQ-D_6 were used as the internal standard for PM2.5, urine, and serum determination, respectively. IS was internal standard. The error bars represent the standard deviation of three repeated measurements.

complex matrices. This derivatization-based wooden-tip ESI-MS has the potential to be applied to environmental monitoring, biomedicine, and clinical diagnosis fields for the rapid determination of quinones with advantages of cheapness, wide accessibility and convenient sampling.

Credit author statement

Chen Ling: Experimental investigation, methodology, data analysis, writing - original draft, **Qiaofang Shi:** Experimental investigation, data analysis, **Zhanpeng Wei:** Data analysis, **Jingjing Zhang:** Writing - review & editing, **Junjie Hu:** Supervision of experiments related to wooden-tip ESI-MS, **Jiying Pei:** Conceptualisation of the wooden-tip ESI-MS method, supervision of experiments, funding acquisition, project administration, writing - review & editing.

Declaration of competing interest

The authors declare that they have no known competing financial interests or personal relationships that could have appeared to influence the work reported in this paper.

Acknowledgments

This work was supported by the National Natural Science Foundation of China (No. 21665003) and the Guangxi Natural Science Fund Project (No. 2018GXNSFAA281354).

Appendix B. Supplementary data

Supplementary data to this article can be found online at https://doi.org/10.1016/j.talanta.2021.122912.

Appendix A. Supplementary data

Supplementary data to this article can be found online at.

References

[1] K.D. Croft, D. Zhang, R. Jiang, A. Ayer, S. Shengule, R.J. Payne, N.C. Ward, R. Stocker, Structural requirements of flavonoids to induce heme oxygenase-1 expression, Free Radic. Biol. Med. 113 (2017) 165–175, https://doi.org/10.1016/j.freeradbiomed.2017.09.030.

[2] L.-E. Cassagnes, P. Perio, G. Ferry, N. Moulharat, M. Antoine, R. Gayon, J. A. Boutin, F. Nepveu, K. Reybier, In cellulo monitoring of quinone reductase activity and reactive oxygen species production during the redox cycling of 1,2 and 1,4 quinones, Free Radic. Biol. Med. 89 (2015) 126–134, https://doi.org/10.1016/j.freeradbiomed.2015.07.150.

[3] Y. Zhao, Q. Xia, J.-J. Yin, H. Yu, P.P. Fu, Photoirradiation of polycyclic aromatic hydrocarbon diones by UVA light leading to lipid peroxidation, Chemosphere 85 (2011) 83–91, https://doi.org/10.1016/j.chemosphere.2011.05.040.

[4] J.L. Bolton, T. Dunlap, Formation and biological targets of quinones: cytotoxic versus cytoprotective effects, Chem. Res. Toxicol. 30 (2017) 13–37, https://doi.org/10.1021/acs.chemrestox.6b00256.

[5] C.A. Jakober, S.G. Riddle, M.A. Robert, H. Destaillats, M.J. Charles, P.G. Green, M. J. Kleeman, Quinone emissions from gasoline and diesel motor vehicles, Environ. Sci. Technol. 41 (2007) 4548–4554, https://doi.org/10.1021/es062967u.

[6] G.F. Shen, S. Tao, W. Wang, Y.F. Yang, J.N. Ding, M.A. Xue, Y.J. Min, C. Zhu, H. Z. Shen, W. Li, B. Wang, R. Wang, W.T. Wang, X.L. Wang, A.G. Russell, Emission of oxygenated polycyclic aromatic hydrocarbons from indoor solid fuel combustion, Environ. Sci. Technol. 45 (2011) 3459–3465, https://doi.org/10.1021/es104364t.

[7] P.P. Fu, Q. Xia, X. Sun, H. Yu, Phototoxicity and environmental transformation of polycyclic aromatic hydrocarbons (PAHs)-light-induced reactive oxygen species, lipid peroxidation, and DNA damage, J. Environ. Sci. Heal. C. 30 (2012) 1–41, https://doi.org/10.1080/10590501.2012.653887.

[8] M. Asahi, M. Kawai, T. Toyama, Y. Kumagai, T. Chuesaard, N. Tang, T. Kameda, K. Hayakawa, A. Toriba, Identification and quantification of in vivo metabolites of 9,10-Phenanthrenequinone in human urine associated with producing reactive oxygen species, Chem. Res. Toxicol. 27 (2014) 76–85, https://doi.org/10.1021/tx400338t.

[9] K. Hayakawa, K. Bekki, M. Yoshita, C. Tachikawa, T. Kameda, N. Tang, A. Toriba, S. Hosoi, Estrogenic/antiestrogenic activities of quinoid polycyclic aromatic hydrocarbons, J. Health Sci. 57 (2011) 274–280, https://doi.org/10.1248/jhs.57.274.

[10] N. Kishikawa, M. Nakao, M.S. Elgawish, K. Ohyama, K. Nakashima, N. Kuroda, 4-Carbomethoxybenzaldehyde as a highly sensitive pre-column fluorescence derivatization reagent for 9,10-phenanthrenequinone, Talanta 85 (2011) 809–812, https://doi.org/10.1016/j.talanta.2011.03.085.

[11] N. Kishikawa, H. Nakashima, K. Ohyama, K. Nakashima, N. Kuroda, Determination of 9, 10-phenanthrenequinone in airborne particulates by high-performance liquid chromatography with post-column fluorescence derivatization using 2-aminothiophenol, Talanta 81 (2010) 1852–1855, https://doi.org/10.1016/j.talanta.2010.03.053.

[12] J.Y.C. Ma, A. Rengasamy, D. Frazer, M.W. Barger, A.F. Hubbs, L. Battelli, S. Tomblyn, S. Stone, V. Castranova, Inhalation exposure of rats to asphalt fumes generated at paving temperatures alters pulmonary xenobiotic metabolism

pathways without lung injury, Environ. Health Perspect. 111 (2003) 1215–1221, https://doi.org/10.1289/ehp.5740.
[13] S. Zhao, H. Jia, G. Nulaji, H. Gao, F. Wang, C. Wang, Photolysis of polycyclic aromatic hydrocarbons (PAHs) on Fe3+-montmorillonite surface under visible light: degradation kinetics, mechanism, and toxicity assessments, Chemosphere 184 (2017) 1346–1354, https://doi.org/10.1016/j.chemosphere.2017.06.106.
[14] L.O. Santos, A.G. Santos, J.B. de Andrade, Methodology to examine polycyclic aromatic hydrocarbons (PAHs) nitrated PAHs and oxygenated PAHs in sediments of the Paraguacu River (Bahia, Brazil), Mar. Pollut. Bull. 136 (2018) 248–256, https://doi.org/10.1016/j.marpolbul.2018.09.022.
[15] I.C. Vaaland, D.M. Pampanin, M.O. Sydnes, Synthesis of trans-dihydronaphthalene-diols and evaluation of their use as standards for PAH metabolite analysis in fish bile by GC-MS, Chemosphere 256 (2020) 126928, https://doi.org/10.1016/j.chemosphere.2020.126928.
[16] K. Luo, S.G. Carmella, Y.C. Zhao, M.K. Tang, S.S. Hecht, Identification and quantification of phenanthrene ortho-quinones in human urine and their association with lipid peroxidation, Environ. Pollut. 266 (2020) 115342, https://doi.org/10.1016/j.envpol.2020.115342.
[17] W. Khan, Y.H. Wang, N.P.D. Nanayakkara, H. Herath, Z. Catchings, S. Khan, P. S. Fasinu, M.A. ElSohly, J.D. McChesney, I.A. Khan, N.D. Chaurasiya, B.L. Tekwani, L.A. Walker, Quantitative determination of primaquine-5,6-ortho-quinone and carboxyprimaquine-5,6-ortho-quinone in human erythrocytes by UHPLC-MS/MS, J. Chromatogr. B. 1163 (2021) 122510, https://doi.org/10.1016/j.jchromb.2020.122510.
[18] Z. Takats, J.M. Wiseman, B. Gologan, R.G. Cooks, Mass spectrometry sampling under ambient conditions with desorption electrospray ionization, Science 306 (2004) 471–473, https://doi.org/10.1126/science.1104404.
[19] R.B. Cody, J.A. Laramee, H.D. Durst, Versatile new ion source for the analysis of materials in open air under ambient conditions, Anal. Chem. 77 (2005) 2297–2302, https://doi.org/10.1021/ac050162j.
[20] H.W. Chen, A. Venter, R.G. Cooks, Extractive electrospray ionization for direct analysis of undiluted urine, milk and other complex mixtures without sample preparation, Chem. Commun. (2006) 2042–2044, https://doi.org/10.1039/b602614a.
[21] P. Nemes, A. Vertes, Laser ablation electrospray ionization for atmospheric pressure, in vivo, and imaging mass spectrometry, Anal. Chem. 79 (2007) 8098–8106, https://doi.org/10.1021/ac071181r.
[22] J.J. Liu, H. Wang, N.E. Manicke, J.M. Lin, R.G. Cooks, Z. Ouyang, Development, characterization, and application of paper spray ionization, Anal. Chem. 82 (2010) 2463–2471, https://doi.org/10.1021/ac902854g.
[23] T.P. Bambauer, H.H. Maurer, A.A. Weber, M. Hannig, N. Putz, M. Koch, S. K. Manier, M. Schneider, M.R. Meyer, Evaluation of novel organosilane modifications of paper spray mass spectrometry substrates for analyzing polar compounds, Talanta 204 (2019) 677–684, https://doi.org/10.1016/j.talanta.2019.05.095.
[24] B. Hu, P.-K. So, H. Chen, Z.-P. Yao, Electrospray ionization using wooden tips, Anal. Chem. 83 (2011) 8201–8207, https://doi.org/10.1021/ac2017713.
[25] B.C. Yang, F.Y. Liu, L.Q. Wang, Y. Zou, F. Wang, W. Deng, X.D. Wan, X. Yang, M. He, O.P. Huang, Serum metabolic profiling study of endometriosis by using wooden-tip electrospray ionization mass spectrometry, Anal. Methods. 7 (2015) 6125–6132, https://doi.org/10.1039/c5ay01312g.
[26] B.C. Yang, F.Y. Liu, J.B. Guo, L. Wan, J. Wu, F. Wang, H. Liu, O.P. Huang, Rapid assay of neopterin and biopterin in urine by wooden-tip electrospray ionization mass spectrometry, Anal. Methods. 7 (2015) 2913–2916, https://doi.org/10.1039/c5ay00004a.
[27] T.T. Ng, P.K. So, B. Hu, Z.P. Yao, Rapid detection and quantitation of drugs-of-abuse by wooden-tip electrospray ionization mass spectrometry, J. Food Drug Anal. 27 (2019) 428–438, https://doi.org/10.1016/j.jfda.2018.09.002.
[28] Y.Y. Yang, J.W. Deng, Internal standard mass spectrum fingerprint: a novel strategy for rapid assessing the quality of Shuang-Huang-Lian oral liquid using wooden-tip electrospray ionization mass spectrometry, Anal. Chim. Acta 837 (2014) 83–92, https://doi.org/10.1016/j.aca.2014.06.005.
[29] B. Hu, Y.Y. Huang, G. Yin, G.F. Zhang, L.Y. Zhang, T.J. Wang, Z.P. Yao, Rapid detection of adulterated drugs in herbal dietary supplements by wooden-tip electrospray ionization mass spectrometry, Anal. Methods. 8 (2016) 6840–6846, https://doi.org/10.1039/c6ay01735e.
[30] J. Deng, Y. Yang, L. Fang, L. Lin, H. Zhou, T. Luan, Coupling solid-phase microextraction with ambient mass spectrometry using surface coated wooden-tip probe for rapid analysis of ultra trace perfluorinated compounds in complex samples, Anal. Chem. 86 (2014) 11159–11166, https://doi.org/10.1021/ac5034177.
[31] Y.H. Liu, Q.X. Yang, X.T. Chen, Y.M. Song, Q.H. Wu, Y.Y. Yang, L.P. He, Sensitive analysis of trace macrolide antibiotics in complex food samples by ambient mass spectrometry with molecularly imprinted polymer-coated wooden tips, Talanta 204 (2019) 238–247, https://doi.org/10.1016/j.talanta.2019.05.102.
[32] G.Z. Xin, B. Hu, Z.Q. Shi, Y.C. Lam, T.T.X. Dong, P. Li, Z.P. Yao, K.W.K. Tsim, Rapid identification of plant materials by wooden-tip electrospray ionization mass spectrometry and a strategy to differentiate the bulbs of Fritillaria, Anal. Chim. Acta 820 (2014) 84–91, https://doi.org/10.1016/j.aca.2014.02.039.
[33] L. Wu, Y.N. Yao, B. Hu, Investigating distributions and changes of alkaloids in living Catharanthus roseus under low-phosphorus stress using wooden-tip electrospray ionisation mass spectrometry, Phytochem. Anal. 31 (2020) 739–746, https://doi.org/10.1002/pca.2937.
[34] Y. Su, H. Wang, J. Liu, P. Wei, R.G. Cooks, Z. Ouyang, Quantitative paper spray mass spectrometry analysis of drugs of abuse, Analyst 138 (2013) 4443, https://doi.org/10.1039/c3an00934c.
[35] J.Y. Pei, C.C. Hsu, Y.H. Wang, K.F. Yu, Corona discharge-induced reduction of quinones in negative electrospray ionization mass spectrometry, RSC Adv. 7 (2017) 43540–43545, https://doi.org/10.1039/c7ra08523k.
[36] X. Zhou, J.Y. Pei, G.M. Huang, Reactive paper spray mass spectrometry for in situ identification of quinones, Rapid Commun. Mass Spectrom. 29 (2015) 100–106, https://doi.org/10.1002/rcm.7092.
[37] M. Liptak, Z. Dinya, C. Nemes, A. Levai, T. Patonay, Electron ionization mass-spectrometry of spiroepoxides generated from e-3-arylideneflavanones, Rapid Commun. Mass Spectrom. 7 (1993) 662–664, https://doi.org/10.1002/rcm.1290070722.
[38] M.T. Le, N.M. Morato, A. Kaerner, C.J. Welch, R.G. Cooks, Fragmentation of polyfunctional compounds recorded using automated high-throughput desorption electrospray ionization, J. Am. Soc. Mass Spectrom. 32 (2021) 2261–2273, https://doi.org/10.1021/jasms.1c00176.
[39] M.J. Sun, W.N. Dai, D.Q. Liu, Fragmentation of aromatic sulfonamides in electrospray ionization mass spectrometry: elimination of SO(2) via rearrangement, J. Mass Spectrom. 43 (2008) 383–393, https://doi.org/10.1002/jms.1335.
[40] J. Bialecki, J. Ruzicka, A.B. Attygalle, An unprecedented rearrangement in collision-induced mass spectrometric fragmentation of protonated benzylamines, J. Mass Spectrom. 41 (2006) 1195–1204, https://doi.org/10.1002/jms.1089.
[41] C. Frontana, A. Vazquez-Mayagoitia, J. Garza, R. Vargas, I. Gonzalez, Substituent effect on a family of quinones in aprotic solvents: an experimental and theoretical approach, J. Phys. Chem. A. 110 (2006) 9411–9419, https://doi.org/10.1021/jp060836+.
[42] J.Y. Pei, C.C. Hsu, R.J. Zhang, Y.H. Wang, K.F. Yu, G.M. Huang, Unexpected reduction of iminoquinone and quinone derivatives in positive electrospray ionization mass spectrometry and possible mechanism exploration, J. Am. Soc. Mass Spectrom. 28 (2017) 2454–2461, https://doi.org/10.1007/s13361-017-1770-4.
[43] E.M. McBride, P.M. Mach, E.S. Dhummakupt, S. Dowling, D.O. Carmany, P. S. Demond, G. Rizzo, N.E. Manicke, T. Glaros, Paper spray ionization: applications and perspectives, Trac. Trends Anal. Chem. 118 (2019) 722–730, https://doi.org/10.1016/j.trac.2019.06.028.
[44] A.K. Jarmusch, V. Pirro, D.L. Logsdon, R.G. Cooks, Direct ion generation from swabs, Talanta 184 (2018) 356–363, https://doi.org/10.1016/j.talanta.2018.02.105.
[45] K. Morand, G. Talbo, M. Mann, Oxidation of peptides during electrospray ionization, Rapid Commun. Mass Spectrom. 7 (1993) 738–743, https://doi.org/10.1002/rcm.1290070811.
[46] B.L. Boys, M.C. Kuprowski, J.J. Noel, L. Konermann, Protein oxidative modifications during electrospray ionization: solution phase electrochemistry or corona discharge-Induced radical attack? Anal. Chem. 81 (2009) 4027–4034, https://doi.org/10.1021/ac900243p.
[47] Z. Zhang, W. Xu, N.E. Manicke, R.G. Cooks, Z. Ouyang, Silica coated paper substrate for paper-spray analysis of therapeutic drugs in dried blood spots, Anal. Chem. 84 (2011) 931–938, https://doi.org/10.1021/ac202058w.
[48] T.H. Kuo, E.P. Dutkiewicz, J.Y. Pei, C.C. Hsu, Ambient ionization mass spectrometry today and tomorrow: embracing challenges and opportunities, Anal. Chem. 92 (2020) 2353–2363, https://doi.org/10.1021/acs.analchem.9b05454.
[49] X.W. Liu, D.E. Sok, Identification of alkylation-sensitive target chaperone proteins and their reactivity with natural products containing Michael acceptor, Arch Pharm. Res. (Seoul) 26 (2003) 1047–1054, https://doi.org/10.1007/bf02994757.
[50] C. Ling, Q.F. Shi, J.J. Zhang, Z.P. Wei, K. Pang, J.Y. Pei, Rapid determination of quinone pollutants in PM2.5 by derivative-based paper spray ionization mass spectrometry, J. Chin. Mass Spectrom. Soc. 42 (2021) 400–410.